Inorg. Chem. **1993**, *32*, 1629-1637

Synthesis and Characterization of Ruthenium Complexes Containing Tridentate $P_3O_9^{3-}$, $Nb_2W_4O_{19}^{4-}$, and $Cp^*TiW_5O_{18}^{3-}$ Ligands

V. W. Day,[*,1a] T. A. Eberspacher,[1a] W. G. Klemperer,[*,1b] R. P. Planalp,[*,1b,c] P. W. Schiller,[1c] A. Yagasaki,[1b] and B. Zhong[1b]

Departments of Chemistry, University of Nebraska, Lincoln, Nebraska 68588, University of Illinois, Urbana, Illinois 61801, and University of New Hampshire, Durham, New Hampshire 03824

Received August 14, 1992

Seven new ruthenium complexes containing tridentate oxygen ligands have been prepared: $[(C_6H_6)Ru(P_3O_9)][N(C_4H_9)_4]$ (**1**), $[(p\text{-cymene})Ru(P_3O_9)][N(C_4H_9)_4]$ (**2**), $[(p\text{-cymene})Ru(Nb_2W_4O_{19})][N(C_4H_9)_4]_2$ (**3**), $[(C_6H_6)Ru(Cp^*TiW_5O_{18})][N(C_4H_9)_4]$ (**4**), $[(CH_3CN)_3Ru(P_3O_9)][N(C_4H_9)_4]\cdot CH_3CN$ (**5**), $[(C_8H_{12})Ru(NH_2NC(CH_3)_2)(P_3O_9)][N(C_4H_9)_4]\cdot CH_3COCH_3$ (**6**), and $[(C_8H_{12})Ru(CH_3CN)(P_3O_9)][N(C_4H_9)_4]\cdot 0.5H_2O$ (**7**). Two of these compounds were structurally characterized using single-crystal X-ray diffraction techniques: compound **5** [a = 24.564(4) Å, b = 9.222(2) Å, c = 15.693(3) Å, Z = 4, space group $Pca2_1\text{-}C^5_{2v}$ (No. 29)] and compound **6** [a = 10.969(2) Å, b = 11.230(2) Å, c = 17.021(3) Å, $\alpha = 74.87(2)°$, $\beta = 74.98(2)°$, $\gamma = 76.18(2)°$, Z = 2, space group $P\bar{1}\text{-}C^1_i$ (No. 2)]. The remaining complexes were formulated and assigned structures on the basis of their elemental composition and the similarity of their infrared spectra and multinuclear NMR spectra with those of isostructural species whose molecular structures have been established crystallographically.

Introduction

Given the ability of ruthenium complexes to mediate oxygen atom transfer reactions[2] and the ability of oxygen ligands to complex high-valent transition metal centers,[3] ruthenium complexes incorporating tridentate oxygen ligands have attracted considerable attention as catalysts or potential catalysts for hydrocarbon oxidations.[4-7] To date, three ligand systems have been employed: Kläui's $(C_5H_5)Co[(RO)_2PO]_3^-$ ligand, R = Me or Et;[5-8] Grim's $C[(C_6H_5)_2PO]_3^-$ ligand;[7] and Tanke's $(C_6H_5)PO(C_6H_4O)_2^{2-}$ ligand.[7] Three new ligands are examined here, namely $P_3O_9^{3-}$, $Nb_2W_4O_{19}^{4-}$, and $Cp^*TiW_5O_{18}^{3-}$, $Cp^* = C_5(CH_3)_5$. These ligands were selected on the basis of their known ability to form stable transition metal complexes.[9-11] Furthermore, the 1,5-cyclooctadiene ligand in the $P_3O_9^{3-}$ complex $[(C_8H_{12})Ir(P_3O_9)]^{2-}$ has been shown to be selectively oxidized by O_2 under ambient reaction conditions.[9g] Our hope in undertaking the present investigation was to develop a similarly reactive ruthenium complex, a hope that has thus far remained unfulfilled.

Results and Discussion

Synthesis and Characterization of (Arene)ruthenium Complexes. The $P_3O_9^{3-}$ ligand reacts as a tetra-n-butylammonium salt with $[(C_6H_6)RuCl_2]_x$[12] in dimethyl sulfoxide[13] and $[(p\text{-cymene})RuCl_2]_2$[12] in chloroform, to form $[(C_6H_6)Ru(P_3O_9)][N(C_4H_9)_4]$ (**1**) and $[(p\text{-cymene})Ru(P_3O_9)][N(C_4H_9)_4]$ (**2**), respectively, where p-cymene is $p\text{-}CH_3C_6H_4CH(CH_3)_2$. As shown in Figure 1a–d, the infrared spectra of **1** and **2** in the P–O stretching region differ from the spectrum of free $P_3O_9^{3-}$ but closely resemble the spectrum of the structurally-characterized complex $[(CH_3CN)_3Ru(P_3O_9)][N(C_4H_9)_4]\cdot CH_3CN$ (see below), known to contain a tridentate $P_3O_9^{3-}$ ligand. This strongly suggests structure a for **1** and an analogous η^6-arene/κ^3O-$P_3O_9^{3-}$ structure

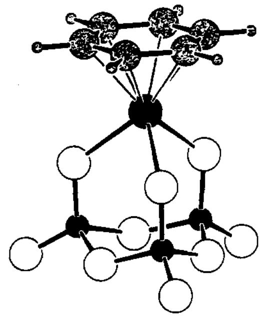

a

---

(1) (a) University of Nebraska. (b) University of Illinois. (c) University of New Hampshire.

(2) Holm, R. H. *Chem. Rev.* **1987**, *87*, 1401.

(3) Griffith, W. P. *The Chemistry of the Rarer Platinum Metals*; Wiley: New York, 1967; p 15.

(4) (Benzene)ruthenium complexes containing the potentially tridentate $P_2W_{15}Nb_3O_{62}^{9-}$ ligand catalyze cyclohexane oxidation, but the constitution and structure of these complexes remains to be established; see: Mizuno, N.; Lyon, D. K.; Finke, R. G. *J. Catal.* **1991**, *128*, 84 and references cited therein (especially ref 18).

(5) (a) Kläui, W. *Angew. Chem., Int. Ed. Engl.* **1990**, *29*, 627. (b) Kläui, W.; Otto, H.; Eberspach, W.; Buchholz, E. *Chem. Ber.* **1982**, *115*, 1922. (c) Kläui, W.; Buchholz, E. *Inorg. Chem.* **1988**, *27*, 3500.

(6) Power, J. M.; Evertz, K.; Henling, L.; Marsh, R.; Schaefer, W. P.; Labinger, J. A.; Bercaw, J. E. *Inorg. Chem.* **1990**, *29*, 5058.

(7) Tanke, R. S.; Holt, E. M.; Crabtree, R. H. *Inorg. Chem.* **1991**, *30*, 1714.

(8) Kolle, U.; Flunkert, G.; Gorissen, R.; Schmidt, M. U.; Englert, U. *Angew. Chem., Int. Ed. Engl.* **1992**, *31*, 440.

(9) $P_3O_9^{3-}$ complexes: (a) Besecker, C. J.; Klemperer, W. G. *J. Organomet. Chem.* **1981**, *205*, C31. (b) Besecker, C. J.; Day, V. W.; Klemperer, W. G. *Organometallics* **1985**, *3*, 564. (c) Day, V. W.; Klemperer, W. G.; Schwartz, C.; Wang, R.-C. In *Surface Organometallic Chemistry: Molecular Approaches to Surface Catalysis*; Basset, J.-M., Gates, B., Candy, J.-P., Choplin, A., Leconte, M., Quignard, F., Santini, C., Eds.; Reidel: Dordrecht, Holland, 1988; p 173. (d) Day, V. W.; Klemperer, W. G.; Lockledge, S. P.; Main, D. J.; Rosenberg, F. S.; Wang, R.-C.; Yaghi, O. M. In *Metal-Metal Bonds in Chemistry and Catalysis*; Fackler, J. P., Ed.; Plenum: New York, 1990; p 161. (e) Day, V. W.; Klemperer, W. G.; Main, D. J. *Inorg. Chem.* **1990**, *29*, 2345. (f) Klemperer, W. G.; Main, D. J. *Inorg. Chem.* **1990**, *29*, 2355. (g) Day, V. W.; Klemperer, W. G.; Lockledge, S. P.; Main, D. J. *J. Am. Chem. Soc.* **1990**, *112*, 2031.

(10) $Nb_2W_4O_{19}^{4-}$ complexes: (a) Besecker, C. J.; Klemperer, W. G. *J. Am. Chem. Soc.* **1980**, *102*, 7598. (b) Besecker, C. J.; Klemperer, W. G.; Day, V. W. *J. Am. Chem. Soc.* **1982**, *104*, 6158. (c) Besecker, C. J.; Day, V. W.; Klemperer, W. G.; Thompson, M. R. *J. Am. Chem. Soc.* **1984**, *106*, 4125. (d) Besecker, C. J.; Day, V. W.; Klemperer, W. G.; Thompson, M. R. *Inorg. Chem.* **1985**, *24*, 44. (e) Reference 9e. (f) Reference 9f.

(11) $Cp^*TiW_5O_{18}^{3-}$ complexes: (a) Klemperer, W. G.; Yagasaki, A. *Chem. Lett.* **1989**, 2041. (b) Che, T. M.; Day, V. W.; Francesconi, L. C.; Klemperer, W. G.; Main, D. J.; Yagasaki, A.; Yaghi, O. M. *Inorg. Chem.* **1992**, *31*, 2920.

(12) Bennett, M. A.; Smith, A. K. *J. Chem. Soc., Dalton Trans.* **1974**, 233.

(13) Ogata, I.; Iwata, R.; Ikeda, Y. *Tetrahedron Lett.* **1970**, 3011.

0020-1669/93/1332-1629$04.00/0

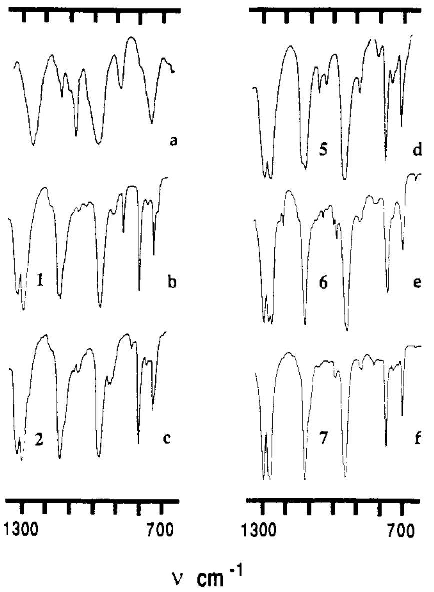

Figure 1. Infrared spectra measured from Nujol mulls of tetra-*n*-butylammonium salts of (a) $P_3O_9^{3-}$, (b) $[(C_6H_6)Ru(P_3O_9)]^-$, (c) $[(p\text{-cymene})Ru(P_3O_9)]^-$, (d) $[(CH_3CN)_3Ru(P_3O_9)]^-$, (e) $[(C_8H_{12})Ru(NH_2NC(CH_3)_2)(P_3O_9)]^-$, and (f) $[(C_8H_{12})Ru(CH_3CN)(P_3O_9)]^-$. For numerical data, see ref 9b for (a) and Experimental section for (b)–(f).

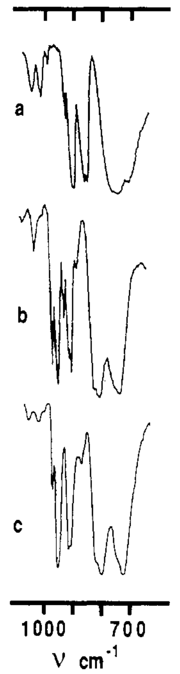

Figure 2. Infrared spectra measured for Nujol mulls of tetra-*n*-butylammonium salts of (a) $Nb_2W_4O_{19}^{4-}$, (b) $[(p\text{-cymene})Ru(Nb_2W_4O_{19})]^{2-}$, and (c) $[Cp^*Rh(Nb_2W_4O_{19})]^{2-}$. For numerical data, see ref 10c for (a) and (c) and Experimental Section for (b).

for **2**. These structures are consistent with ^1H and ^{31}P NMR data given in the Experimental Section. Both **1** and **2** are air-stable as solids and in CH_3CN solutions under ambient conditions. While **1** is very sparingly soluble in 1,2-dichloroethane and acetone, **2** is soluble in these solvents and in CH_2Cl_2 as well.

Reaction of *cis*-$Nb_2W_4O_{19}^{4-}$ as a tetra-*n*-butylammonium salt with $[(p\text{-cymene})RuCl_2]_2$ in 1,2-dichloroethane yields $[(p\text{-cymene})Ru(Nb_2W_4O_{19})][N(C_4H_9)_4]_2$ (**3**). The product, isolated as yellow rod-shaped crystals, is air-stable as a solid as well as in methylene chloride, chloroform, 1,2-dichloroethane and acetonitrile solution under ambient conditions. The infrared spectrum of **3** in the 650–1050-cm^{-1} metal–oxygen stretching region (Figure 2b) is quite different from that of the free $Nb_2W_4O_{19}^{4-}$ ligand[14] (Figure 2a), but closely resembles the spectrum of the structurally-characterized $[(\eta^5\text{-}C_5Me_5)Rh(\kappa^3O\text{-}cis\text{-}Nb_2W_4O_{19})]^{2-}$ anion[10c] (Figure 2c), suggesting analogous κ^3O-*cis*-$Nb_2W_4O_{19}^{4-}$ coordination in **3**, where a set of three contiguous doubly-bridging $Nb_2W_4O_{19}^{4-}$ oxygens are coordinated to the Ru^{II} center. Three diastereomeric $[(C_5Me_5)Rh(Nb_2W_4O_{19})]^{2-}$ isomers having this structure are known,[10c] and since infrared spectroscopy does not provide clear fingerprints for the isomeric structures, NMR spectroscopy was used to establish the number of isomers and identity of the isomers present. The ^{13}C NMR spectrum of **3** (see the Experimental Section) showed the presence of two different *p*-cymene groups and hence two of the three possible diastereomers. The ^{17}O NMR spectrum of **3** (see Figure 3) showed an ONb_2Ru resonance plus five OW_2 resonances, a result identifying the isomers present as the two shown at the top of Figure 3 (see ref 10c).

The $Cp^*TiW_5O_{18}^{3-}$ ion does not react with $[(C_6H_6)RuCl_2]_x$ under the conditions employed for the synthesis of $[(C_6H_6)Ru(P_3O_9)]^-$ from $P_3O_9^{3-}$ plus $[(C_6H_6)RuCl_2]_x$. Its tetra-*n*-butylammonium salt does, however, react with the $[(C_6H_6)Ru(CH_3CN)_3]^{2+}$ cation in noncoordinating solvents such as 1,2-dichloroethane to form $[(C_6H_6)Ru(Cp^*TiW_5O_{18})][N(C_4H_9)_4]$ (**4**). This compound is insoluble in all but the most polar organic solvents, and is only slightly soluble in CH_3CN, CH_3NO_2, $(CH_3)_2NCHO$, and $(CH_3)_2SO$ (ca. 4 mg/mL). It is stable toward O_2 under ambient conditions both in solution and the solid state. As shown in Figure 4, compound **4** and $[(C_8H_{12})Ir(Cp^*TiW_5O_{18})][N(C_4H_9)_4]_2$[11a] have very similar infrared spectra in the 600–1000-cm^{-1} region, suggesting similar binding modes for the $Cp^*TiW_5O_{18}^{3-}$ ligand. Structure b is therefore proposed for the anion of **4**, a structure analogous to that established by single-crystal X-ray diffraction studies for the $[(C_8H_{12})Ir(Cp^*TiW_5O_{18})]^{2-}$ anion.

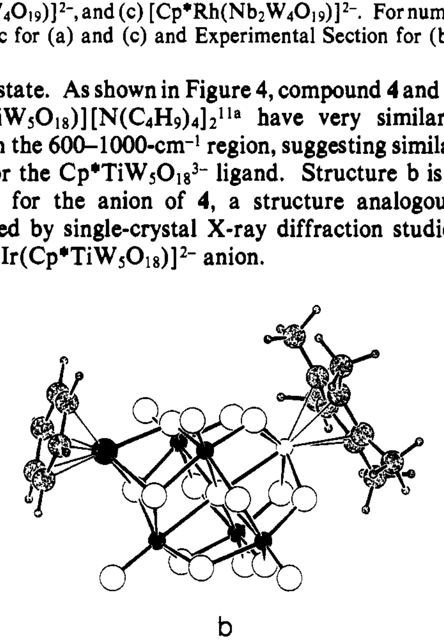

b

Photolysis of (Arene)ruthenium Complexes. Photolysis of $[(C_6H_6)Ru(P_3O_9)][N(C_4H_9)_4]$ (**1**), in CH_3CN for 25 h under conditions described in the Experimental Section produced a single product in >90% yield according to ^{31}P NMR spectroscopy. This material could be isolated in 73% yield as yellow, needle-shaped, air-stable crystals and identified as $[(CH_3CN)_3Ru(P_3O_9)][N(C_4H_9)_4]\cdot CH_3CN$ (**5**) by elemental analysis, infrared spectroscopy, and ^{31}P as well as ^1H NMR spectroscopy.

X-ray structural analysis (see Table I) revealed that single crystals of compound **5** are composed of discrete octahedral $[(CH_3CN)_3Ru(P_3O_9)]^-$ anions (Table II and Figure 5), $N(C_4H_9)_4^+$ cations (Figure S1a[15]), and acetonitrile solvent molecules of crystallization (Figure S1b[15]). Although the anion of **5** possesses no rigorous crystallographic symmetry in the solid state, it approximates rather closely its maximum possible site symmetry of C_{3v} with one set of octahedral *fac* sites being occupied by the three coordinated CH_3CN ligands and the other set of *fac*

---

[14] Rocchiccioli-Deltcheff, C.; Thouvenot, R.; Dabbabi, M. *Spectrochim. Acta, Part A* 1977, *33A*, 143.

[15] See paragraph at the end of paper regarding supplementary material.

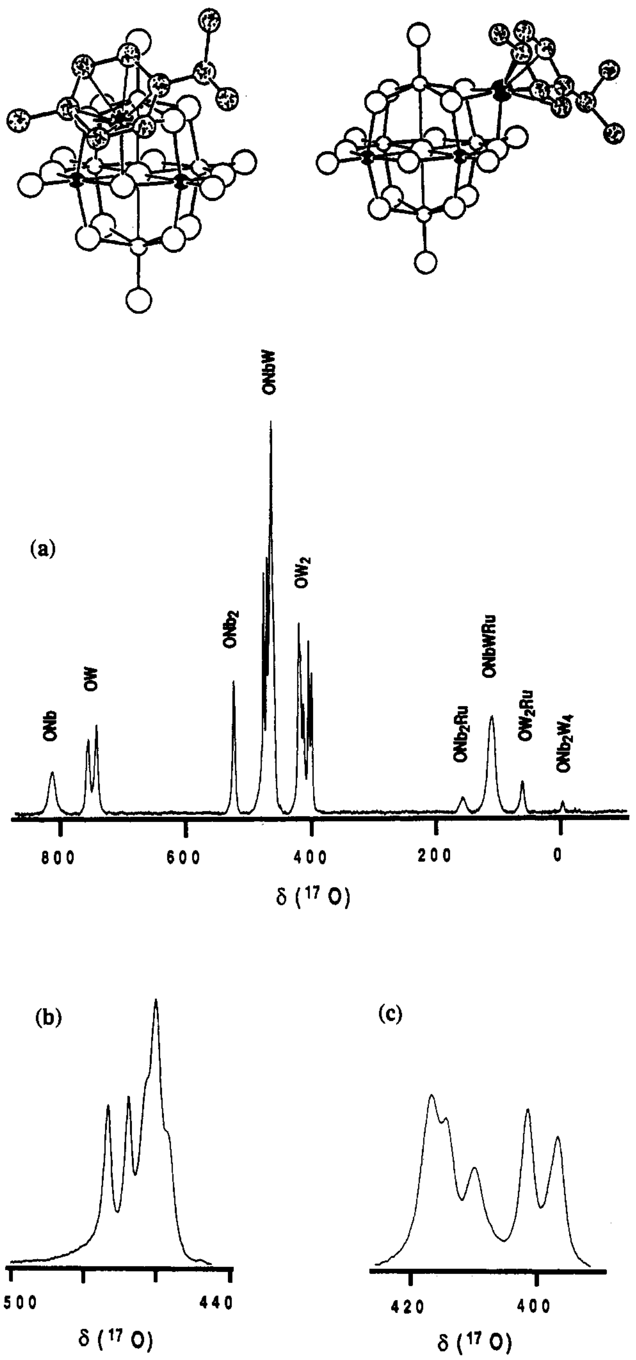

Figure 3. Top: SCHAKAL drawings of the two isomeric structures proposed for the $[(p\text{-cymene})Ru(Nb_2W_4O_{19})]^{2-}$ anion in compound 3. Hydrogen atoms are not shown, and niobium atoms are represented by small filled circles, tungsten atoms by small open circles, oxygen atoms by large open circles, carbon atoms by large shaded circles, and ruthenium atoms by large filled circles. Bottom: Complete ^{17}O NMR spectrum of compound 3 (a), plus horizontal expansions of the 450–500 ppm ONbW (b) and 380–430 ppm OW_2 (c) regions. See Experimental Section for spectral parameters and numerical data.

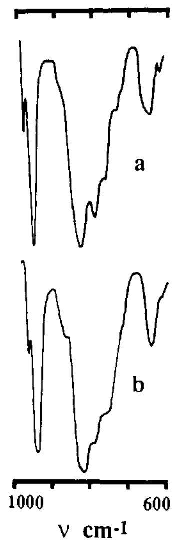

Figure 4. Infrared spectra of (a) $[(C_6H_6)Ru(Cp^*TiW_5O_{18})][N(C_4H_9)_4]$ and (b) $[(C_8H_{12})Ir(Cp^*TiW_5O_{18})][N(C_4H_9)_4]_2$ measured from Nujol mulls between KBr plates. For numerical data, see Experimental Section for (a) and ref 11a for (b).

Table I. Crystallographic Data for $[(CH_3CN)_3Ru(P_3O_9)][N(C_4H_9)_4]\cdot CH_3CN$ (**5**) and $[(C_8H_{12})Ru(NH_2NC(CH_3)_2)(P_3O_9)][N(C_4H_9)_4]\cdot CH_3COCH_3$ (**6**)

	5	**6**
formula	$RuC_{24}H_{48}N_5O_9P_3$	$RuC_{30}H_{62}N_3O_{10}P_3$
fw	744.65	818.81
space group[28]	$Pca2_1\text{-}C^5_{2v}$ (No. 29)	$P\bar{1}\text{-}C^1_i$ (No. 2)
cell constants		
a, Å	24.564(4)	10.969(2)
b, Å	9.222(2)	11.230(2)
c, Å	15.693(3)	17.021(3)
α, deg	90.0	74.87(2)
β, deg	90.0	74.98(2)
γ, deg	90.0	76.18(2)
V, $Å^3$	3554.9(6)	1921.6(4)
Z	4	2
ρ_{calcd}, g cm^{-3}	1.391	1.415
T, °C	20 ± 1	-75 ± 3
μ, mm^{-1} [26c]	0.63	0.59
transm coeff	0.675–1.000	0.936–0.966
radiation	Mo K$\bar{\alpha}$	Mo K$\bar{\alpha}$
$R(F_o)$[25]	0.042	0.045
$R_w(F_o)$[25]	0.048	0.054

sites by coordinated O_c oxygens on the three phosphorus atoms of a single $\kappa^3\text{-}O\text{-}P_3O_9^{3-}$ ligand. The nine oxygen atoms of the trimetaphosphate anion are distributed among three distinct structural types: three bridging O_b oxygens which are bonded to two phosphorus atoms, three coordinated O_c oxygens which are bonded to Ru and one phosphorus, and three O_t oxygens which are terminally-bonded to a single phosphorus atom.

The bond lengths and angles in the $[(CH_3CN)_3Ru(P_3O_9)]^-$ anion (Table III) are rather unexceptional. The average[16] bond lengths are: Ru–N, 1.973(9,13,19,3) Å; Ru–O_c, 2.116–(7,6,9,3) Å; (acetonitrile) C≡N, 1.130(15,4,7,3) Å; (acetonitrile) C–C, 1.471(18,5,7,3) Å; P–O_c, 1.500(8,6,9,3) Å; P–O_b, 1.616(8,7,20,6) Å; and P–O_t, 1.455(8,1,2,3) Å. The average[16] bond angles are: O_cRuO_c, 89.9(3,4,5,3)°; NRuN, 90.9(4,19,29,3)°, *cis* O_c-RuN, 89.6(3,11,21,6)°; *trans* O_cRuN, 178.2(3,7,10,3)°; RuNC, 175.5(10,21,32,3)°; NCC, 177.5(15,11,16,3)°; RuO_cP, 122.3(5,3,5,3)°; PO_bP, 123.7(5,5,7,3)°; O_cPO_b, 108.3(4,3,7,3)°; O_bPO_b, 100.2(4,1,1,3)°; O_cPO_t, 118.8(5,2,4,3)°; and O_bPO_t, 109.8(5,4,7,6)°. Bond lengths and angles in the cation[15] and acetonitrile solvent molecule of crystallization[15] of **5** are normal.

The $[(CH_3CN)_3Ru(P_3O_9)]^-$ anion in **5** is a very stable complex. It is stable toward oxygen under ambient conditions in solution and the solid state. A solution of **5** in CD_3CN shows no exchange of bound acetonitrile with solvent acetonitrile at 25 °C according to ^1H NMR spectroscopy. When exposed to UV light (medium-pressure Hg arc lamp, 450-W, Pyrex filter) for 0.5 h, however, exchange of solvent acetonitrile with bound acetonitrile is complete.

When the $[(p\text{-cymene})Ru(P_3O_9)]^-$ salt **2** was photolyzed under the same conditions used to prepare **5** from **1**, less than 25%

---

(16) The first number in parentheses following an average value of a bond length or angle is the root-mean-square estimated standard deviation of an individual datum. The second and third numbers are the average and maximum deviations from the average value, respectively. The fourth number represents the number of individual measurements which are included in the average value.

Table II. Atomic Coordinates for Atoms in the Anion of Crystalline $[(CH_3CN)_3Ru(P_3O_9)][N(C_4H_9)_4]\cdot CH_3CN$ (**5**)[a]

atom	fractional coord			equiv isotropic
type[b]	10^4x	10^4y	10^4z	thermal param, *B*, Å² × 10[c]
Ru	1304(1)	1129(1)	0[d]	29(1)
P_1	1910(1)	3595(3)	1045(2)	33(1)
P_2	789(1)	4092(3)	655(2)	32(1)
P_3	1086(1)	2038(3)	1931(2)	31(1)
O_{1b}	1405(3)	4663(8)	782(5)	35(2)
O_{2b}	694(3)	3284(8)	1557(4)	32(2)
O_{3b}	1664(3)	2865(8)	1892(4)	32(2)
O_{1c}	1965(3)	2455(8)	377(4)	34(2)
O_{2c}	788(3)	2952(6)	−29(6)	35(2)
O_{3c}	1097(3)	805(7)	1301(4)	34(2)
O_{1t}	2385(3)	4456(8)	1268(6)	46(2)
O_{2t}	426(4)	5329(9)	578(5)	43(2)
O_{3t}	937(4)	1727(9)	2811(5)	47(3)
N_1	692(4)	−131(10)	−291(5)	31(2)
N_2	1796(4)	−570(9)	6(8)	37(2)
N_3	1507(4)	1480(11)	−1209(6)	35(2)
C_{11}	327(5)	−871(12)	−392(7)	38(3)
C_{12}	−136(5)	−1859(14)	−470(8)	45(4)
C_{21}	2083(5)	−1526(11)	20(12)	45(3)
C_{22}	2449(6)	−2785(13)	−12(14)	66(4)
C_{31}	1651(5)	1785(15)	−1864(8)	43(4)
C_{32}	1844(8)	2165(23)	−2729(10)	85(6)
H_{12a}	−347	−2021	−975	54
H_{12b}	−376	−1724	6	54
H_{12c}	94	−2682	−368	54
H_{22a}	2512	−3097	562	79
H_{22b}	2785	−2450	−255	79
H_{22c}	2312	−3582	−340	79
H_{32a}	1882	3101	−2978	102
H_{32b}	1524	1706	−2952	102
H_{32c}	2159	1594	−2863	102

[a] The numbers in parentheses are the estimated standard deviations in the last significant digit. [b] Atoms are labeled in agreement with Figure 5. [c] For non-hydrogen atoms, this is one-third of the trace of the orthogonalized $\mathbf{B}_{ij}$ tensor; for hydrogen atoms, it is the assigned value for the isotropic thermal parameter. [d] This atom was used to fix the origin of the unit cell along the $\vec{c}$-axis, and this coordinate is therefore listed without an estimated standard deviation.

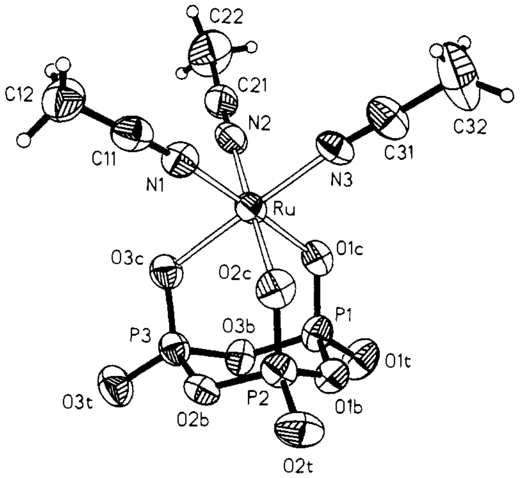

Figure 5. Perspective drawing of the $[(CH_3CN)_3Ru(P_3O_9)]^-$ anion present in crystalline $[(CH_3CN)_3Ru(P_3O_9)][N(C_4H_9)_4]\cdot CH_3CN$ (**5**). All non-hydrogen atoms are represented by thermal vibration ellipsoids drawn to encompass 50% of their electron density; hydrogen atoms are represented by small spheres which are in no way representative of their true thermal motion.

conversion to **5** was obtained. The $[(p\text{-cymene})Ru(Nb_2W_4O_{19})]^{2-}$ anion in **3** and the $[(C_6H_6)Ru(Cp^*TiW_5O_{18})]^-$ anion in **4** were even less reactive, yielding no measurable amounts of product under similar photolysis conditions. Efforts to prepare $[(CH_3CN)_3Ru(Nb_2W_4O_{19})]^{2-}$ and $[(CH_3CN)_3Ru(Cp^*TiW_5O_{18})]^-$ directly from the appropriate polyoxanion plus $Ru(CH_3CN)_6^{2+}$[17] were equally unsuccessful, even at elevated temperatures.

Table III. Bond Lengths and Angles Involving Non-Hydrogen Atoms in the Anion of Crystalline $[(CH_3CN)_3Ru(P_3O_9][N(C_4H_9)_4]\cdot CH_3CN$ (**5**)[a]

param[b]	value	param[b]	value
	Bond Lengths (Å)		
Ru–N_1	1.954(9)	Ru–O_{1c}	2.117(8)
Ru–N_2	1.978(8)	Ru–O_{2c}	2.107(6)
Ru–N_3	1.988(9)	Ru–O_{3c}	2.125(7)
P_1–O_{1c}	1.491(8)	P_1–O_{1b}	1.636(8)
P_2–O_{2c}	1.502(9)	P_1–O_{3b}	1.608(8)
P_3–O_{3c}	1.508(8)	P_2–O_{1b}	1.614(8)
P_1–O_{1t}	1.455(8)	P_2–O_{2b}	1.616(8)
P_2–O_{2t}	1.454(9)	P_3–O_{3b}	1.612(8)
P_3–O_{3t}	1.457(8)	P_3–O_{2b}	1.610(8)
N_1–C_{11}	1.137(16)	C_{11}–C_{12}	1.464(18)
N_2–C_{21}	1.130(14)	C_{21}–C_{22}	1.470(17)
N_3–C_{31}	1.124(15)	C_{31}–C_{32}	1.478(20)
	Bond Angles (deg)		
$O_{1c}RuN_2$	89.3(3)	$O_{1c}RuN_3$	88.8(3)
$O_{2c}RuN_1$	90.4(3)	$O_{2c}RuN_3$	90.0(4)
$O_{3c}RuN_1$	87.5(3)	$O_{3c}RuN_2$	91.7(4)
$O_{1c}RuO_{2c}$	90.4(3)	N_1RuN_2	90.0(4)
$O_{1c}RuO_{3c}$	89.8(3)	N_1RuN_3	93.8(4)
$O_{2c}RuO_{3c}$	89.4(3)	N_2RuN_3	88.9(5)
$O_{1c}RuN_1$	177.2(3)	$O_{2c}RuN_2$	178.9(4)
$O_{3c}RuN_3$	178.5(3)		
RuN_1C_{11}	174.4(9)	$N_1C_{11}C_{12}$	176.5(12)
RuN_2C_{21}	178.7(11)	$N_2C_{21}C_{22}$	176.8(19)
RuN_3C_{31}	173.4(10)	$N_3C_{31}C_{32}$	179.1(13)
$RuO_{1c}P_1$	122.2(5)	$P_1O_{1b}P_2$	123.0(5)
$RuO_{2c}P_2$	122.8(5)	$P_1O_{3b}P_3$	124.1(5)
$RuO_{3c}P_3$	121.9(4)	$P_2O_{2b}P_3$	124.1(5)
$O_{1b}P_2O_{2b}$	100.3(4)	$O_{1c}P_1O_{1t}$	118.8(5)
$O_{1b}P_1O_{3b}$	100.1(4)	$O_{2c}P_2O_{2t}$	119.2(5)
$O_{3b}P_3O_{2b}$	100.1(4)	$O_{3c}P_3O_{3t}$	118.5(5)
$O_{1c}P_1O_{1b}$	108.4(4)	$O_{1b}P_1O_{1t}$	109.9(4)
$O_{1c}P_1O_{3b}$	108.7(4)	$O_{1b}P_2O_{2t}$	109.3(5)
$O_{2c}P_2O_{1b}$	108.6(4)	$O_{2b}P_2O_{2t}$	110.2(4)
$O_{2c}P_2O_{2b}$	107.6(4)	$O_{2b}P_3O_{3t}$	109.6(5)
$O_{3c}P_3O_{2b}$	108.0(4)	$O_{3b}P_1O_{1t}$	109.3(5)
$O_{3c}P_3O_{3b}$	108.4(4)	$O_{3b}P_3O_{3t}$	110.5(5)

[a] The numbers in parentheses are the estimated standard deviations in the last significant digit. [b] Atoms are labeled in agreement with Figure 5.

Synthesis and Characterization of (Cyclooctadiene)ruthenium Complexes. Reaction of the cyclooctadiene complex $[(C_8H_{12})Ru(N_2H_4)_4][B(C_6H_5)_4]_2$[18] with $(P_3O_9)[N(C_4H_9)_4]_3$ in acetone yielded a yellow, crystalline, air-stable product, $[(C_8H_{12})Ru(NH_2NC(CH_3)_2)(P_3O_9)][N(C_4H_9)_4]\cdot CH_3COCH_3$ (**6**), according to analytical and spectroscopic data given below in the Experimental Section. X-ray structural analysis (see Table I) revealed that single crystals of compound **6** are composed of discrete $[(C_8H_{12})Ru(NH_2NC(CH_3)_2)(P_3O_9)]^-$ anions (Table IV and Figure 6), $N(C_4H_9)_4^+$ cations (Figure S2a[15]), and acetone solvent molecules of crystallization (Figure S2b[15]). The d^6 Ru^{2+} ion in the anion of **6** achieves an 18-electron valence shell configuration by being π-bonded to the two olefinic bonds of a single 1,5-cyclooctadiene ligand, σ-bonded to the amine nitrogen of an acetone hydrazone moiety, and σ-bonded to three terminal oxygens on different phosphorus atoms of a single $P_3O_9^{3-}$ ligand. Two *cis* coordination sites of the octahedral Ru^{2+} coordination sphere in the anion of **6** are occupied by the midpoints of the two olefinic C=C bonds (designated as C_{g12} and C_{g56}, respectively), three *fac* sites are occupied by the coordinated O_c oxygens of the trimetaphosphate ligand and the sixth coordination site is occupied by the amino nitrogen of the coordinated acetone hydrazone ligand.

---

(17) Rapaport, I.; Helm, L.; Merbach, A. E.; Bernhard, P.; Ludi, A. *Inorg. Chem.* **1988**, *27*, 873.

(18) Ashworth, T. V.; Singleton, E.; Hough, J. J. *J. Chem. Soc., Dalton Trans.* **1977**, 1809.

Table IV. Atomic Coordinates for Atoms in the Anion of Crystalline $[(C_8H_{12})Ru(NH_2NC(CH_3)_2)(P_3O_9)][N(C_4H_9)_4]\cdot CH_3COCH_3$ (**6**)[a]

atom	fractional coord			equiv isotropic
type[b]	10^4x	10^4y	10^4z	thermal param B, Å^2 × 10[c]
Ru	1854(1)	3054(1)	1021(1)	14(1)
P_1	1274(3)	3937(3)	2790(2)	21(1)
P_2	−535(3)	5067(3)	1762(2)	18(1)
P_3	−424(3)	2505(3)	2636(2)	19(1)
O_{1b}	270(6)	5135(6)	2399(4)	20(2)
O_{2b}	−1202(6)	3877(6)	2250(4)	19(2)
O_{3b}	340(6)	2923(6)	3190(4)	19(2)
O_{1c}	2241(6)	3509(6)	2082(4)	20(2)
O_{2c}	398(6)	4745(5)	996(4)	14(2)
O_{3c}	536(6)	2024(6)	1942(4)	16(2)
O_{1t}	1691(7)	4259(7)	3442(4)	28(3)
O_{2t}	−1518(6)	6220(6)	1641(4)	23(2)
O_{3t}	−1339(6)	1735(6)	3177(4)	22(2)
N_1	854(9)	2821(9)	175(6)	18(3)
N_2	399(8)	1655(8)	374(5)	18(3)
C_1	3502(10)	1630(10)	1268(7)	24(4)
C_2	3030(10)	1313(10)	684(6)	21(3)
C_3	3573(10)	1538(10)	−239(7)	29(4)
C_4	3882(10)	2834(9)	−632(7)	26(4)
C_5	3018(9)	3852(9)	−181(6)	16(3)
C_6	3302(9)	4198(10)	480(6)	18(3)
C_7	4521(10)	3587(10)	804(7)	28(4)
C_8	4733(10)	2163(10)	1042(7)	27(4)
C_9	−799(10)	1687(10)	662(6)	21(4)
C_{10}	−1844(10)	2806(10)	826(7)	30(4)
C_{11}	−1224(11)	433(10)	932(7)	32(4)
H_{1Na}	1151(101)	3045(106)	−416(72)	40(30)[d]
H_{1Nb}	316(83)	3336(85)	129(56)	4(24)[d]
H_1	3037	1508	1836	30
H_2	2292	915	886	23
H_{3a}	4349	936	−337	37
H_{3b}	2957	1411	−505	37
H_{4a}	4758	2815	−624	33
H_{4b}	3778	3047	−1198	33
H_5	2235	4278	−360	21
H_6	2708	4840	734	22
H_{7a}	4480	3895	1288	35
H_{7b}	5239	3827	379	35
H_{8a}	5292	1839	579	35
H_{8b}	5136	1890	1513	35
H_{10a}	−2669	2565	958	37
H_{10b}	−1748	3395	301	37
H_{10c}	−1779	3187	1253	37
H_{11a}	−2099	476	1231	39
H_{11b}	−680	−216	1243	39
H_{11c}	−1146	248	399	39

[a] The numbers in parentheses are the estimated standard deviations in the last significant digit. [b] Atoms are labeled in agreement with Figure 6. [c] For non-hydrogen atoms, this is one-third of the trace of the orthogonalized $\mathbf{B}_{ij}$ tensor; for hydrogen atoms bonded to carbon, it is the assigned value for the isotropic thermal parameter. [d] For hydrogen atoms H_{1Na} and H_{1Nb}, this is the refined value of the isotropic thermal parameter.

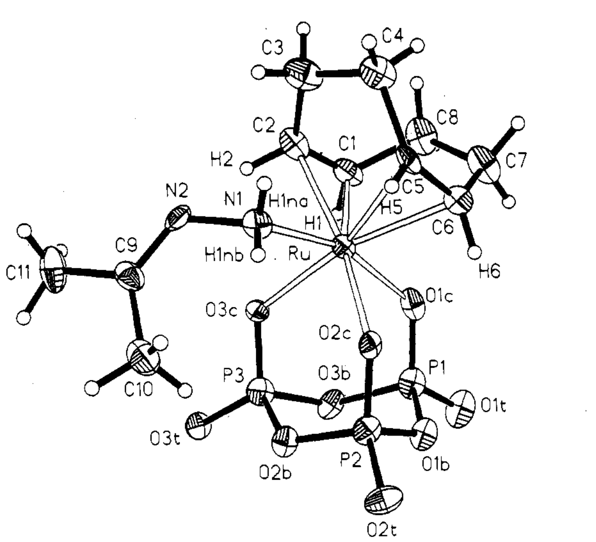

Figure 6. Perspective drawing of the $[(C_8H_{12})Ru(NH_2NC(CH_3)_2)(P_3O_9)]^-$ anion present in crystalline $[(C_8H_{12})Ru(NH_2NC(CH_3)_2)(P_3O_9)][N(C_4H_9)_4]\cdot CH_3COCH_3$ (**6**). All non-hydrogen atoms are represented by thermal vibration ellipsoids drawn to encompass 50% of their electron density; hydrogen atoms are represented by small spheres which are in no way representative of their true thermal motion.

The bond lengths and angles for the 1,5-cyclooctadiene ligand (Table V) are normal and those in the acetone hydrazone ligand are quite similar to those previously observed for this ligand.[19] The average[16] bond lengths and angles within the $P_3O_9{}^{3-}$ ligand of **6** are very similar to those observed in **5**: P–O_c, 1.492(6,7,10,3) Å; P–O_b, 1.618(8,13,26,6) Å; P–O_t, 1.464(7,10,15,3) Å; PO_bP, 123.1(4,7,10,3)°; O_bPO_c, 108.0(4,3,7,6)°; O_bPO_b, 100.6(4,8,11,3)°; O_cPO_t, 118.8(4,13,19,3)° and O_bPO_t, 109.9(4,5,9,6)°. The ~0.04 Å longer 2.156(7,13,20,3) Å average[16] Ru–O_c bond length in **6** relative to **5** is presumably the result of the excellent π-bonding abilities of a cyclooctadiene ligand and its greater steric bulk relative to two acetonitriles.

The choice of an octahedral description for the coordination geometry of Ru in **6** is clearly indicated by the average bond angles subtended at Ru involving the midpoints of the olefinic cyclooctadiene bonds (C_{g12} and C_{g56}): O_cRuO_c, 86.6(3,24,35,3)°; C_gRuC_g,[20] 86.9°; C_gRuN_1,[20] 97.6(-,8,8,2)°; *cis* O_cRuN_1, 82.1(3,24,22,2)°; *cis* O_cRuC_g,[20] 93.7(-,22,29,4)°; *trans* O_cRuN_1, 161.3(3)°; and *trans* O_cRuC_g,[20] 177.8(-,9,9,2)°. Nonetheless, it is obvious that two η^2-coordinated olefin moieties will occupy a larger area on the Ru coordination sphere in **6** than the two corresponding nitrogens (N_2 and N_3) in **5**. The "effective" coordination number for Ru in **6** is therefore somewhat greater than six and the Ru-to-ligand bonds for similar ligands (i.e., $P_3O_9{}^{3-}$) would be expected to be longer in **6** than in **5** (as the data in Tables III and V indicate). Even though the Ru coordination sphere in **6** is larger than in **5**, the ligand···ligand contacts listed in Table VI indicate that the Ru coordination sphere in **6** is quite congested. Whereas the range of values for each type of short contact on the Ru coordination sphere is small for **5**, it is large for **6**. Ranges for the various types of contacts in **5** are: O···O, 2.98–3.00 Å; N···O, 2.82–2.95 Å; and N···N, 2.78–2.88 Å. Ranges for contacts in **6** are: O···O, 2.87–3.05 Å; N···O, 2.75–2.86 Å, C···O, 2.66–3.16 Å; H···O, 2.31–2.72 Å; C···N, 2.75–2.77 Å; H···N, 2.34–2.56 Å; and C···C, 2.83–2.85 Å. When compared to the van der Waals values[21] of 2.80 Å for O···O, 2.90 Å for N···O, 3.00 Å for N···N, 3.10 Å for C···O, 2.60 Å for H···O, 3.20 Å for C···N, 2.70 Å for H···N, and 3.40 Å for C···C, short contacts on these Ru coordination spheres are seen to be much more numerous and severe in **6** than **5**.

Bond lengths and angles in the cation[15] and acetone solvent molecule of crystallization[15] of **6** are normal. The anions of **6** form hydrogen-bonded dimers (Figure 7) in the crystal. Amino hydrogen atom H_{1Na} is involved in an intermolecular hydrogen bond with the terminal O_{2t} oxygen of a symmetry-related ($\bar{x}$, 1 − y, $\bar{z}$) molecule; the $N_1 \cdots O_{2t}$ distance is 2.95 Å and the N_1–$H_{1Na} \cdots O_{2t'}$ angle is 170°.

Another air-stable (cyclooctadiene)ruthenium complex could be prepared from $P_3O_9{}^{3-}$ and $[(C_8H_{12})Ru(CH_3CN)_4](PF_6)_2$[22] in CH_3NO_2. Although no products were observed at ambient

---

(19) (a) Nolte, M. J.; Singleton, E. *J. Chem. Soc., Dalton Trans.* **1974**, 2406. (b) Hausen, H. D.; Krogmann, K. *Z. Anorg. Allg. Chem.* **1972**, *389*, 247.

(20) C_g is used to designate the midpoint of a cyclooctadiene olefinic bond. These values are therefore listed without an estimated standard deviation.

(21) Pauling, L. *The Nature of the Chemical Bond*, 3rd ed.; Cornell University Press: Ithaca, NY, 1960; p 260.

(22) (a) Albers, M. O.; Ashworth, T. V.; Oosthuizen, E.; Singleton, E. *Inorg. Synth.* **1989**, *26*, 68. (b) Ashworth, T. V.; Singleton, E. *J. Organomet. Chem.* **1974**, *77*, C31. (c) Schrock, R. R.; Johnson, B. F. G.; Lewis, J. *J. Chem. Soc., Dalton Trans.* **1974**, 951.

Table V. Bond Lengths and Angles Involving Non-Hydrogen Atoms in the Anion of Crystalline $[(C_8H_{12})Ru(NH_2NC(CH_3)_2)(P_3O_9)][N(C_4H_9)_4]\cdot CH_3COCH_3$ (**6**)[a]

param[b]	value	param[b]	value
	Bond Lengths (Å)		
$Ru–O_{1c}$	2.164(8)	$Ru–C_1$	2.160(10)
$Ru–O_{2c}$	2.168(6)	$Ru–C_2$	2.194(10)
$Ru–O_{3c}$	2.136(6)	$Ru–C_5$	2.203(8)
$Ru–N_1$	2.121(13)	$Ru–C_6$	2.150(11)
$P_1–O_{1c}$	1.486(7)	$P_1–O_{1b}$	1.635(7)
$P_2–O_{2c}$	1.502(6)	$P_1–O_{3b}$	1.613(7)
$P_3–O_{3c}$	1.487(6)	$P_2–O_{1b}$	1.592(9)
$P_1–O_{1t}$	1.457(9)	$P_2–O_{2b}$	1.608(7)
$P_2–O_{2t}$	1.479(6)	$P_3–O_{3b}$	1.624(9)
$P_3–O_{3t}$	1.456(7)	$P_3–O_{2b}$	1.633(6)
$C_1–C_2$	1.387(19)	$C_5–C_6$	1.408(17)
$C_2–C_3$	1.506(14)	$C_6–C_7$	1.520(15)
$C_3–C_4$	1.513(15)	$C_7–C_8$	1.519(15)
$C_4–C_5$	1.536(14)	$C_8–C_1$	1.525(16)
$N_1–N_2$	1.439(14)	$C_9–C_{10}$	1.517(14)
$N_2–C_9$	1.274(13)	$C_9–C_{11}$	1.508(17)
	Bond Angles (deg)		
$O_{1c}RuO_{2c}$	85.7(3)	$O_{1c}RuN_1$	161.3(3)
$O_{1c}RuO_{3c}$	83.9(3)	$O_{2c}RuC_1$	163.1(4)
$O_{2c}RuO_{3c}$	90.1(2)	$O_{2c}RuC_2$	159.5(4)
		$O_{3c}RuC_5$	162.2(4)
$O_{2c}RuN_1$	79.7(3)	$O_{3c}RuC_6$	160.0(4)
$O_{3c}RuN_1$	84.4(3)		
$O_{1c}RuC_1$	78.1(4)	$O_{1c}RuC_2$	114.7(3)
$O_{3c}RuC_1$	93.2(3)	$O_{1c}RuC_5$	113.8(4)
		N_1RuC_1	117.1(4)
N_1RuC_2	80.0(4)	N_1RuC_6	115.2(4)
N_1RuC_5	78.8(4)		
C_1RuC_5	89.4(3)	$O_{3c}RuC_2$	90.9(3)
C_2RuC_5	80.7(3)	$O_{2c}RuC_5$	92.4(3)
C_1RuC_6	82.0(4)	$O_{2c}RuC_6$	89.2(3)
C_2RuC_6	96.7(4)	$O_{1c}RuC_6$	76.1(3)
C_1RuC_2	37.1(5)	C_5RuC_6	37.7(4)
$C_{g12}RuC_{g56}$[c]	86.9(-)	$C_{g12}RuN_1$[c]	98.4(-)
		$C_{g56}RuN_1$[c]	96.8(-)
$RuO_{1c}P_1$	126.6(4)	$P_1O_{1b}P_2$	123.2(5)
$RuO_{2c}P_2$	123.1(3)	$P_1O_{3b}P_3$	122.1(4)
$RuO_{3c}P_3$	125.6(4)	$P_2O_{2b}P_3$	124.1(4)
$O_{1b}P_2O_{2b}$	101.7(4)	$O_{1c}P_1O_{1t}$	119.9(4)
$O_{1b}P_1O_{3b}$	100.2(4)	$O_{2c}P_2O_{2t}$	116.9(4)
$O_{3b}P_3O_{2b}$	99.8(4)	$O_{3c}P_3O_{3t}$	119.6(4)
$O_{1c}P_1O_{1b}$	107.3(4)	$O_{1b}P_1O_{1t}$	109.0(4)
$O_{1c}P_1O_{3b}$	108.3(4)	$O_{1b}P_2O_{2t}$	110.1(4)
$O_{2c}P_2O_{1b}$	107.9(4)	$O_{2b}P_2O_{2t}$	110.5(4)
$O_{2c}P_2O_{2b}$	108.5(4)	$O_{2b}P_3O_{3t}$	109.3(4)
$O_{3c}P_3O_{2b}$	108.1(3)	$O_{3b}P_1O_{1t}$	110.4(4)
$O_{3c}P_3O_{3b}$	108.1(4)	$O_{3b}P_3O_{3t}$	110.0(4)
RuN_1N_2	115.9(7)		
RuC_1C_8	112.4(7)	RuC_1C_2	72.8(6)
RuC_2C_3	109.9(6)	RuC_2C_1	70.1(6)
RuC_5C_4	112.3(6)	RuC_5C_6	69.1(5)
RuC_6C_7	110.4(6)	RuC_6C_5	73.2(6)
$C_2C_1C_8$	122.4(9)	$C_4C_5C_6$	124.0(9)
$C_1C_2C_3$	125.8(10)	$C_5C_6C_7$	122.0(9)
$C_2C_3C_4$	115.1(10)	$C_6C_7C_8$	114.4(10)
$C_3C_4C_5$	113.2(8)	$C_1C_8C_7$	113.9(8)
$N_1N_2C_9$	117.3(8)	$N_2C_9C_{10}$	128.6(11)
$N_2C_9C_{11}$	115.7(9)	$C_{10}C_9C_{11}$	115.5(9)

[a] The numbers in parentheses are the estimated standard deviations in the last significant digit. [b] Atoms are labeled in agreement with Figure 6. [c] C_{g12} and C_{g56} are used to denote the midpoint of the $C_1{=}C_2$ and $C_5{=}C_6$ olefinic bonds, respectively, and these values are therefore listed without estimated standard deviations.

Table VI. Close Contacts (Å) between Coordinated Atoms on the Ru Coordination Spheres in $[(CH_3CN)_3Ru(P_3O_9)][N(C_4H_9)_4]\cdot CH_3CN$ (**5**) and $[(C_8H_{12})Ru(NH_2NC(CH_3)_2)(P_3O_9)][N(C_4H_9)_4]\cdot CH_3COCH_3$ (**6**)

contact[a]	dist (Å)	contact[a]	dist (Å)
$O_{1c}\cdots O_{2c}$	3.00	$O_{1c}\cdots O_{2c}$	2.95
$O_{1c}\cdots O_{3c}$	2.99	$O_{1c}\cdots O_{3c}$	2.87
$O_{2c}\cdots O_{3c}$	2.98	$O_{2c}\cdots O_{3c}$	3.05
$N_1\cdots O_{2c}$	2.88	$N_1\cdots O_{2c}$	2.75
$N_1\cdots O_{3c}$	2.82	$N_1\cdots O_{3c}$	2.86
$N_2\cdots O_{1c}$	2.88	$C_1\cdots O_{1c}$	2.73
		$H_1\cdots O_{1c}$	2.31
$N_2\cdots O_{3c}$	2.95	$C_1\cdots O_{3c}$	3.12
		$H_1\cdots O_{3c}$	2.63
		$C_2\cdots O_{3c}$	3.09
		$H_2\cdots O_{3c}$	2.59
$N_3\cdots O_{1c}$	2.87	$C_6\cdots O_{1c}$	2.66
		$H_6\cdots O_{1c}$	2.39
$N_3\cdots O_{2c}$	2.90	$C_5\cdots O_{2c}$	3.16
		$H_5\cdots O_{2c}$	2.72
		$C_6\cdots O_{2c}$	3.03
		$H_6\cdots O_{2c}$	2.48
$N_1\cdots N_2$	2.78	$C_2\cdots N_1$	2.77
		$H_2\cdots N_1$	2.56
$N_1\cdots N_3$	2.88	$C_5\cdots N_1$	2.75
		$H_5\cdots N_1$	2.34
$N_2\cdots N_3$	2.78	$C_1\cdots C_6$	2.83
		$C_2\cdots C_5$	2.85

[a] Atoms are labeled in agreement with Tables II–V and Figures 5 and 6.

temperature, the reaction proceeded almost quantitatively at 68 °C, according to ^{31}P and ^1H NMR monitoring experiments. The product, compound **7**, was identified as $[(C_8H_{12})Ru(CH_3CN)(P_3O_9)][N(C_4H_9)_4]\cdot 0.5H_2O$ and assigned the anion structure c on the basis of the following evidence. First, elemental analysis was consistent with this formulation. Second, ^1H NMR spectra were consistent with the proposed formulation, displaying resonances for four methine protons, eight methylene protons, and three methyl protons in addition to the appropriate number of cation resonances. Third, ^{31}P NMR spectroscopy showed an A_2X pattern with parameters very similar to those observed for compound **6** ($\delta = -9.41$ (t, 1P), $\delta = -6.75$ (d, 2P), $J = 21.0$ Hz for **7**; $\delta = -9.89$ (t, 1P), $\delta = -7.50$ (d, 2P), $J = 21.7$ Hz for **6**). Finally, the infrared spectrum of compound **7** in the 650–1350-cm^{-1} region (Figure 1f) was extremely similar to the spectrum of compound **6** in the same region (Figure 1e), supporting a similar structural environment for the $P_3O_9{}^{3-}$ ligand.

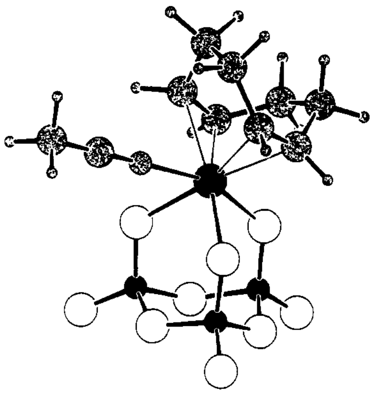

C

Efforts to prepare $Cp^*TiW_5O_{18}{}^{3-}$ and $Nb_2W_4O_{19}{}^{4-}$ complexes of $(C_8H_{12})Ru^{II}$ from $[(C_8H_{12})Ru(N_2H_4)_4]^{2+}$ and $[(C_8H_{12})Ru(CH_3CN)_4]^{2+}$ were unsuccessful.

Experimental Section

Reagents, Solvents, and General Procedures. Unless stated otherwise, all operations were conducted under an atmosphere of prepurified nitrogen. The following were purchased from commercial sources and used without further purification: α-phellandrene (Pfaltz and Bauer); $RuCl_3\cdot 3H_2O$ (Aesar); 1,3-cyclohexadiene (Aldrich); *m*-chloroperbenzoic acid (Aldrich); chloroform (Fisher); absolute ethanol (USI Chemicals); and dimethyl sulfoxide (Aldrich, absolute grade). Acetone (Fisher) was dried with Linde type 4A molecular sieves and then distilled; 1,2-dichloroethane was stored over Linde type 3A molecular sieves. Molecular sieves were activated by maintaining at 350 °C for 24 h and cooling to ambient temperature under vacuum. Nitromethane (Baker) was dried over $CaCl_2$

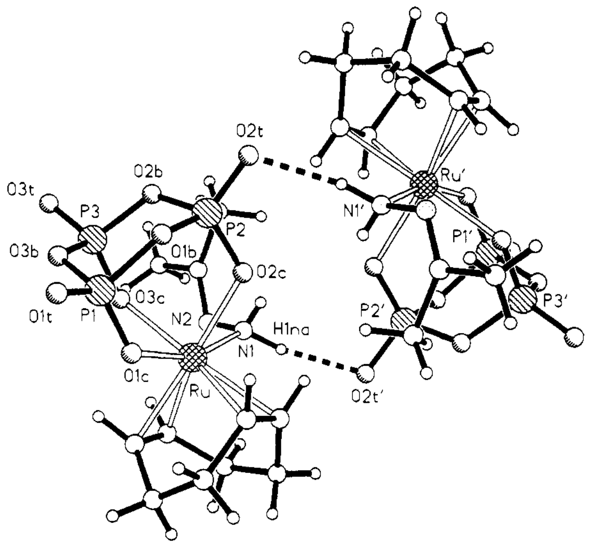

Figure 7. Perspective drawing of the dimeric hydrogen-bonded $[(C_8H_{12})Ru(NH_2NC(CH_3)_2)(P_3O_9)]_2^{2-}$ moieties present in crystalline $[(C_8H_{12})Ru(NH_2NC(CH_3)_2)(P_3O_9)][N(C_4H_9)_4]\cdot CH_3COCH_3$ (**6**). Ru and P atoms are represented by crosshatched and striped large spheres; O, N, and C atoms are represented by shaded, dotted, and open medium-sized spheres, respectively. Hydrogen atoms are represented by small open spheres. Atoms labeled with a prime (′) are related to those labeled without a prime by the crystallographic inversion center at (0,1,0) in the unit cell. Hydrogen bonds are shown with dashed lines.

and then distilled. Diethyl ether (Mallinckrodt, anhydrous), acetonitrile (Burdick and Jackson), and methylene chloride (Fisher) were distilled from Na/K alloy, CaH_2, and P_4O_{10}, respectively. Preparation and ^{17}O enrichment of $(Nb_2W_4O_{19})[N(C_4H_9)_4]_4$ was achieved using procedures described in ref 10c; $(P_3O_9)[N(C_4H_9)_4]_3\cdot 2.5H_2O$,[9b] $(Cp^*TiW_5O_{18})[N(C_4H_9)_4]_3$,[11b] $[(C_6H_6)RuCl_2]_x$,[12] $[(p\text{-cymene})RuCl_2]_2$,[12] $[(C_8H_{12})Ru(CH_3CN)_4](PF_6)_2$,[22a] $[(C_8H_{12})Ru(N_2H_4)_4][B(C_6H_5)_4]_2$,[21] and $[(C_6H_6)Ru(CH_3CN)_3](PF_6)_2$[23] were prepared according to literature procedures.

Analytical Procedures. Elemental analyses were performed by the School of Chemical Sciences Microanalytical Laboratory at the University of Illinois.

Infrared spectra were measured from mineral oil (Nujol) mulls between KBr plates on a Perkin-Elmer 1330 spectrometer and were references to the 1028-cm^{-1} band of a 0.05-mm polystyrene film. Absorptions are described as follows: strong (s), medium (m), weak (w), shoulder (sh), and broad (br).

^1H FTNMR spectra were recorded on a 300-MHz General Electric QE-300 spectrometer and referenced internally to tetramethylsilane. All of the compounds were $(n\text{-}C_4H_9)_4N^+$ salts, and their cation resonances, not reported below, appeared as multiplets centered at about 3.2, 1.7, 1.4, and 1.0 ppm. Resonances are described as follows: singlet (s), doublet (d), triplet (t), and multiplet (m).

^{17}O FTNMR spectra were measured at 40.7 MHz in 10-mm o.d. vertical sample tubes without sample spinning on an unlocked General Electric GN-300 WB spectrometer. A spectral bandwidth of 40 000 Hz was digitized using 8192 data points. The pulse repetition rate was 9.71 Hz, and the pulse width employed, 43 μs, corresponded to a 90° pulse. A preacquisition delay time of 25 ms was used. Chemical shift values were externally referenced to 22 °C fresh tap water using the sample replacement method. Reported line widths have been corrected for the 10-Hz exponential line-broadening employed.

$^{31}P\{^1H\}$ FTNMR spectra were measured at 121.5 MHz on a General Electric GN-300 NB spectrometer equipped with a deuterium lock. The pulse repetition rate was 0.4 Hz. A spectral bandwidth of 1689 Hz was digitized using 16 384 data points. Chemical shifts were externally referenced to 85% aqueous H_3PO_4 using the sample replacement method.

Chemical shift values for all nuclear magnetic resonances are reported as positive numbers for resonances observed at higher frequency (lower field) than the relevant reference resonance.

Preparation of $[(C_6H_6)Ru(P_3O_9)][N(C_4H_9)_4]$ (1). Dimethyl sulfoxide (18 mL) was added to $[(C_6H_6)RuCl_2]_x$ (1.0 g, 4.0 mmol) and the mixture was stirred for 40 min to obtain a deep red solution. The solution was suction filtered and $(P_3O_9)[N(C_4H_9)_4]_3\cdot 2.5H_2O$ (4.0 g, 4.0 mmol) was added with stirring. The solid was completely dissolved after 5 min, yielding a red-brown solution. Diethyl ether (200 mL) was added with vigorous stirring, yielding a yellow-brown paste and a yellow supernatant. The supernatant was then decanted, and the paste was washed three times with 140 mL of diethyl ether, with vigorous stirring. The resulting sticky solid was then dissolved in acetonitrile (30 mL) and 75 mL of diethyl ether was carefully layered over this solution. Large, red-orange crystals appeared after 24 h at ambient temperature. The supernatant was then decanted and the crystals were washed with 10 mL of diethyl ether and dried in vacuum for 30 min. The yield was 1.85 g (2.81 mmol, 70% based on Ru). Anal. Calcd for $C_{22}H_{42}NO_9P_3Ru$: C, 40.12; H, 6.43; N, 2.13; P, 14.11; Ru, 15.35. Found: C, 40.17; H, 6.41; N, 2.17; P, 14.08; Ru, 15.15. IR (Nujol, 700–1325 cm^{-1}; see Figure 1b): 700 (w, sh), 713 (m), 742 (w), 774 (s), 847 (m), 893 (w, br), 944 (s, br), 1012 (w), 1043 (w), 1102 (m, sh), 1120 (s), 1130 (s), 1168 (w, sh), 1280 (s), 1306 (s) cm^{-1}. ^1H NMR (CD_3CN, 25 °C, 0.015 M): δ 5.71 (s). $^{31}P\{^1H\}$ NMR (CD_3CN, 25 °C, 0.015 M): δ −5.89(s).

Preparation of $[(p\text{-cymene})Ru(P_3O_9)][N(C_4H_9)_4]$ (2). An orange solution of $[(p\text{-cymene})RuCl_2]_2$ (1.2 g, 1.96 mmol) in chloroform (7 mL) was added to a solution of $(P_3O_9)[N(C_4H_9)_4]_3\cdot 2.5H_2O$ (4.1 g, 4.1 mmol) in chloroform (10 mL) with stirring, to yield an orange solution which in some cases yielded a yellow precipitate after 5–10 s. Diethyl ether (35 mL) was then added to the reaction mixture, producing a mass of sticky, yellow crystals. These crystals were isolated by filtration, washed with diethyl ether (3 × 40 mL), dried for 10 min under vacuum, and then dissolved in 30 mL of chloroform. This orange solution was filtered and then cooled to −10 °C, giving yellow needles which were isolated by filtration, dissolved in chloroform (30 mL), and recrystallized by diffusion of diethyl ether (40 mL) into the solution. The yellow prisms and needles which formed were isolated by filtration and recrystallized again from acetonitrile/diethyl ether (10 mL/15 mL), yielding 2.32 g of yellow-orange crystals (3.25 mmol, 83% based on Ru). Anal. Calcd for $C_{26}H_{50}NRuP_3O_9$: C, 43.61; H, 7.05; N, 1.96; Ru, 14.14; P, 13.00. Found: C, 43.61; H, 7.04; N, 1.92; Ru, 14.19; P, 12.88. IR (Nujol, 700–1325 cm^{-1}; see Figure 1c): 710 (m), 729 (w), 743 (w), 771 (s), 809 (w), 888 (sh), 897 (m), 907 (m), 941 (s), 1040 (w, br), 1059 (w), 1094 (sh)), 1115 (s), 1259 (sh), 1285 (s), 1306 (s) cm^{-1}. ^1H NMR ($CDCl_3$, 25 °C): δ 5.49 (d, *J* = 6 Hz, C_6H_4), 5.23 (d, *J* = 6 Hz, C_6H_4), 3.00 (m, $CH(CH_3)_2$), 1.36 (d, *J* = 7 Hz, $CH(CH_3)_2$), 2.24 (s, CH_3). $^{31}P\{^1H\}$ NMR (CD_3CN, 25 °C, 0.015 M): δ −6.37.

Preparation of $[(p\text{-cymene})Ru(Nb_2W_4O_{19})][N(C_4H_9)_4]_2$ (3). A solution of $[(p\text{-cymene})RuCl_2]_2$ (0.14 g, 0.23 mmol) in 1,2-dichloroethane (2 mL) was added to a solution of $(Nb_2W_4O_{19})[N(C_4H_9)_4]_4$ (1.0 g, 0.46 mmol) in 1,2-dichloroethane (2 mL) with stirring. After 3 h, diethyl ether (450 mL) was added to the red-orange reaction solution with stirring, producing a yellow oil and a golden brown supernatant. After 18 h stirring, a yellow solid had separated from the oil, and a few brown crystals had formed from the mixture. These solids and the oil were scraped against the wall of the reaction vessel to give a dark green solid, the supernatant was decanted, and the solid was washed with 50 mL of diethyl ether. After decanting the diethyl ether, the solid was redissolved in 4 mL of $CHCl_3$, reprecipitated with 100 mL of ether, isolated by filtration, dried in vacuum for 30 min, and dissolved in 6 mL of acetonitrile. A layer of ether (4 mL) was carefully placed over this solution, and the mixture was stored at −10 °C for 18 h. The supernatant was then decanted, and the crystals that had formed were washed with ether (20 mL) and dried in vacuum. Final purification was accomplished by redissolving the crystals in 5 mL of acetonitrile and diffusing 4 mL of diethyl ether into this solution. The yield was 0.30 g (0.154 mmol, 33% based on Ru). Anal. Calcd for $C_{42}H_{86}N_2Nb_2O_{19}RuW_4$: C, 25.93; H, 4.46; N, 1.44; Nb, 9.55; Ru, 5.20; W, 37.80. Found: C, 25.76; H, 4.48; N, 1.46; Nb, 9.46; Ru, 5.30; W, 37.90. IR (Nujol, 700–1000 cm^{-1}; see Figure 2b): 735 (s, br), 758 (sh, br), 810 (s, br), 827 (sh, br), 885 (w), 916 (s), 924 (s), 958 (s), 979 (m) cm^{-1}. ^1H NMR (CD_3CN, 25 °C): δ 5.91 (d, *J* = 6 Hz, C_6H_4), 5.85 (d, *J* = 6 Hz, C_6H_4), 5.84 (d, *J* = 6 Hz, C_6H_4), 5.78 (d, *J* = 6 Hz, C_6H_4), 2.42 (s, $C_6H_4CH_3$), 2.38 (s, $C_6H_4CH_3$), 1.43 (d, $C_6H_4CH(CH_3)_2$), 1.41 (d, $C_6H_4(CH_3)_2$). The two methine resonances are obscured by the δ 3.2 cation resonance. ^{17}O NMR ((0.05 M in CH_3CN, 17 at % ^{17}O, 22 °C, 5000 acquisitions; see Figure 3): δ 813 (ONb), 754, 753, 740 (OW); 521 (ONb_2); 473, 468, 463, 460, 457 (ONbW); 417, 415, 410, 401, 397 (OW_2); 153 ($ORuNb_2$); 106 (ORuNbW); 58 ($ORuW_2$); −7 (ONb_2W_4).

---

[23] The PF_6^- salt of $[(C_6H_6)Ru(CH_3CN)_3]^{2+}$ was prepared by following the procedure given for the BF_4^- salt in ref 12, but replacing $AgBF_4$ with an equivalent amount of $AgPF_6$.

Preparation of [$(C_6H_6)Ru(Cp^*TiW_5O_{18})$][$N(C_4H_9)_4$] (4). A suspension of [$(C_6H_6)Ru(CH_3CN)_3$]$(PF_6)_2$ (0.58 g, 0.98 mmol) in a solution of ($Cp^*TiW_5O_{18}$)[$N(C_4H_9)_4$]$_3$ (2.0 g, 0.94 mmol) in 60 mL of 1,2-dichloroethane yielded a cloudy yellow-orange solution and a yellow-orange precipitate after stirring for 17 h. Addition of 160 mL of diethyl ether generated additional precipitate, and all the solids in the reaction vessel were collected by filtration, washed with 2 × 20 mL diethyl ether, and dried for 3 h under vacuum to generate 1.21 g of crude product. This material was dissolved in 53 mL of boiling CH_3CN, and the resulting solution was filtered while hot. After the filtrate had cooled to ambient temperature, 110 mL of diethyl ether was added with stirring, causing precipitation of yellow-orange microcrystalline powder. Two hours later, this material was collected by filtration, washed with 2 × 20 mL of diethyl ether, and dried under vacuum at ca. 60 °C for 8 h. The yield was 0.99 g (0.55 mmol, 58% based on W). Anal. Calcd for $C_{32}H_{57}NO_{18}RuTiW_5$: C, 21.21; H, 3.17; N, 0.77; Ru, 5.58; Ti, 2.64; W, 50.73. Found: C, 21.19; H, 3.16; N, 0.78; Ru, 5.69; Ti, 2.59; W, 50.61. IR (Nujol, 600–1000 cm^{-1}; see Figure 4a): 625 (w), 652 (m), 667 (sh), 740 (sh), 774 (sh), 799 (s), 837 (s), 961 (s), 987 (m) cm^{-1}. ^1H NMR (CD_3CN, 25 °C): δ 6.02 (s, C_6H_6), 2.00 (s, $C_5(CH_3)_5$).

Preparation of [$(CH_3CN)_3Ru(P_3O_9)$][$N(C_4H_9)_4$]·CH_3CN (5). A solution of [$(C_6H_6)Ru(P_3O_9)$][$N(C_4H_9)_4$] (2.5 g, 3.8 mmol) in 75 mL of acetonitrile was irradiated with a medium-pressure Hg arc lamp (450 W, Canrad-Hanovia) for 25 h, causing the solution to change its color from orange to yellow. The reaction solution was then filtered, and 150 mL of diethyl ether was carefully layered over the filtrate. Large pale-yellow, needle-shaped crystals appeared in the course of 2 days, and these crystals were collected by filtration, washed with ether, and dried in vacuum to yield 2.07 g of product (2.78 mmol, 73%). The same product was obtained when crystals were obtained by gaseous diffusion of diethyl ether into an acetonitrile solution, but under these conditions both needle- and plate-shaped crystals were obtained simultaneously. Anal. Calcd for $C_{24}H_{48}N_5O_9P_3Ru$: C, 38.71; H, 6.50; N, 9.40; P, 12.48; Ru, 13.57. Found: C, 38.50; H, 6.43; N, 9.26; P, 12.41; Ru, 13.55. IR (Nujol, 700–1325 cm^{-1}; see Figure 1d): 702 (s), 727 (sh, br), 741 (m), 766 (s), 806 (W, br), 885 (m), 947 (s, br), 1031 (m), 1063 (m), 1116 (s), 1133 (s, br), 1272 (s), 1297 (s) cm^{-1}. ^1H NMR (CD_3CN, 25 °C): δ 2.59. $^{31}P\{^1H\}$ NMR (CD_3CN, 25 °C, 0.015 M): δ –4.48.

Preparation of [$(C_8H_{12})Ru(NH_2NC(CH_3)_2)(P_3O_9)$][$N(C_4H_9)_4$]·$CH_3COCH$ (6). A solution of [$(COD)Ru(N_2H_4)_4$]$(BPh_4)_2$ (4.0 g, 4.1 mmol) in 110 mL of acetone was added dropwise to a refluxing solution of $P_3O_9(TBA)_3$·$2.5H_2O$ (4.53 g, 4.49 mmol) in 640 mL of acetone with rapid stirring over a period of 15 min. The resulting yellow solution was refluxed for an hour, and then filtered to remove a trace amount of colorless crystalline precipitate. The filtrate was concentrated under reduced pressure to 130 mL, causing precipitation of a yellow crystalline solid. After the reaction mixture was allowed to stand at –20 °C for 8 h, the yellow product was rapidly collected by filtration, washed with 3 × 15 mL of an acetone/ether mixture (1/2 v/v), and dried in vacuum for 12 h. Yield was 2.35 g (2.87 mmol, 70% based on Ru). Anal. Calcd for $C_{30}H_{62}N_3O_{10}P_3Ru$: C, 44.01; H, 7.63; N, 5.13; P, 11.35; Ru, 12.34. Found: C, 43.76; H, 7.60; N, 5.22; P, 11.22; Ru, 11.91. IR (Nujol, 700–1350 cm^{-1}; see Figure 1e): 707 (s), 749 (w, sh), 773 (s), 823 (w, br), 890 (m, br), 946 (s), 988 (m), 902 (m), 1025 (w), 1045 (w), 1073 (w), 1123 (s), 1214 (m), 1229 (w, sh), 1264 (s), 1277 (s), 1296 (s) cm^{-1}. ^1H NMR (CD_3NO_2, 25 °C): δ 1.91–2.07 (m, CH_2, 4H), 2.06 (s, CMe_2, 3H), 2.08 (s, CMe_2, 3H), 2.11 (s, CH_3COCH_3, 6H), 2.32–2.53 (m, CH_2, 4H), 3.76–3.87 (m, CH, 2H), 3.95–4.06 (m, CH, 2H), 7.12 (s, br, NH_2, 2H). ^{31}P NMR (CD_3NO_2, 0.026 M, 25 °C): δ –9.89 (t, *J* = 21.6 Hz, 1P), –7.50 (d, *J* = 21.7 Hz, 2P).

Preparation of [$(C_8H_{12})Ru(CH_3CN)(P_3O_9)$][$N(C_4H_9)_4$]·$0.5H_2O$ (7). A solution of [$(C_8H_{12}Ru(CH_3CN)_4$]$(PF_6)_2$ (0.20 g, 0.30 mmol) and (P_3O_9)[$N(C_4H_9)_4$]$_3$·$2.5H_2O$ (0.31 g, 0.31 mmol) in 6 mL of CH_3NO_2 was heated at 68 °C for 3 h to produce a light yellow-brown solution containing a trace amount of pale yellow powder, which was removed by filtration. The filtrate was concentrated under a reduced pressure to 2.5 mL, and mixed with 30 mL of diethyl ether. The resulting pale yellow and white crystalline precipitate and a small amount of brown sticky material, collected by decanting off the colorless supernatant, were washed with 3 × 10 mL of ether. The wet solid was washed successively with 2-mL portions of THF with stirring until the wash became colorless: at this point, the brown, sticky material and colorless crystals of [$N(C_4H_9)_4$](PF_6) were completely washed away. The remaining pale yellow crystalline solid was washed with ether and dried in vacuum at ca. 55 °C overnight to afford 0.17 g of slightly hygroscopic product (0.23 mmole, 77% based on Ru). Anal. Calcd for $C_{26}H_{51}N_2O_9P_3Ru$·$0.5H_2O$: C, 42.28; H, 7.10; N, 3.79; P, 12.58; Ru, 13.68. Found: C, 42.29; H, 7.18; N, 3.76; P, 12.35; Ru, 13.35. IR (Nujol, 700–1325 cm^{-1}; see Figure 1f): 704 (s), 746 (w), 774 (s), 829 (w), 885 (m), 948 (s), 995 (m), 1071 (w), 1125 (s), 1275 (s), 1284 (sh), 1305 (s) cm^{-1}. ^1H NMR (CD_3NO_2, 25 °C): δ 1.93–2.04 (m, CH_2, 4H), 2.32–2.54 (m, CH_2, 4H), 2.76 (s, CH_3CN, 3H), 3.96–4.12 (m, CH, 4H). ^{31}P NMR (CD_3NO_2, 0.05 M, 25 °C): δ –9.41 (t, *J* = 21.0 Hz, 1P), –6.75 (d, *J* = 21.0 Hz, 2P).

X-ray Crystallographic Studies[15] of [$(CH_3CN)_3Ru(P_3O_9)$][$N(C_4H_9)_4$]·CH_3CN (5) and [$(C_8H_{12})Ru(NH_2NC(CH_3)_2(P_3O_9)$][$N(C_4H_9)_4$]·$CH_3COCH_3$ (6). Plate-shaped single crystals of compound **5**, obtained as described above, and rectangular parallelepiped-shaped crystals of **6**, which were grown by slow evaporation of an acetone solution at ambient temperature, were suitable for X-ray diffraction studies. Details of the structure determinations for **5** and **6** are summarized in Table I.

Totals of 4139 (**5**) and 5323 (**6**) independent reflections having 2*θ*(Mo K*α*) < 55° (**5**) or 46° (**6**) were collected at 20 ± 1 °C (**5**) or –75 ± 3 °C (**6**) on a computer-controlled Nicolet autodiffractometer (**5**) or Enraf-Nonius CAD4 automated *κ*-axis diffractometer (**6**) in concentric shells of increasing 2*θ* using 1.10°-wide *ω* scans (**5**) or *θ*–2*θ* scans which were (1.5 + 0.52 tan *θ*)° wide (**6**) and graphite-monochromated Mo K$\bar{\alpha}$ radiation for nearly rectangular-parallelepiped-shaped specimens with dimensions of 0.32 × 0.35 × 0.50 mm (**5**) and 0.06 × 0.18 × 0.22 mm (**6**). The crystal of **5** was sealed with mother liquor inside a thin-walled glass capillary and the crystal of **6** was mounted, using oil, on the end of a thin glass fiber. The crystal of **5** was mounted on the diffractometer with its longest edge nearly parallel to the phi axis and the crystal of **6** was mounted with the (0,1,0) scattering planes nearly perpendicular to the spindle axis of the diffractometer. Fixed scanning rates of 6°/min or 4°/min were used for the various shells of data for **5** and variable scanning rates of 3°/min to 16°/min were used for **6**. The data collection and reduction procedures that were used for **5** are described in detail elsewhere.[10c] In the present study of **5**, counts were accumulated for 15 equal time intervals during the scan and those 13 contiguous intervals that had the highest single accumulated count at their midpoint were used to calculate the net intensity; the scan width and step-off for background measurements were both 1.10° in the present study and the ratio of total background counting time to net scanning time was 0.50. The intensity data for both compounds were corrected empirically (**5**) or numerically (**6**) for variable absorption effects; *ψ* scans for six reflections having 2*θ* between 5.19° and 29.06° were used in the empirical correction for **5**. The metal and phosphorus atoms of both compounds were located using "heavy-atom" Patterson techniques (**5**) or (SHELXTL) "direct methods" techniques (**6**) and counter-weighed[24] full-matrix least-squares refinement of the structural parameters for the one anisotropic Ru and three anisotropic P atoms of each compound gave *R*[25] (unweighted, based on *F*) = 0.241 (**5**) and 0.292 (**6**) for 2204 (**5**) and 2711 (**6**) independent absorption-corrected reflections having $I > 3\sigma(I)$ and 2*θ*(Mo K*α*) < 55° (**5**) or 46° (**6**). A series of difference Fourier syntheses based on increasingly more complete structural models for both compounds revealed all of the remaining non-hydrogen and most of the hydrogen atoms in the asymmetric units of both compounds. The amino hydrogen atoms of **6** were refined as individual isotropic atoms. The methyl groups of the three coordinated acetonitrile ligands in **5** and all eight methyl groups in **6** were refined as rigid rotors with idealized sp^3-hybridized geometry and a C–H bond length of 0.96 Å. The methylene hydrogens for the cations of both compounds and the cyclooctadiene hydrogens for **6** were included in the structural model as fixed atoms at idealized positions (assuming sp^2- or sp^3-hybridization of the carbon atom and a C–H bond length of 0.96 Å). The isotropic thermal parameter of each included hydrogen atoms (except amino hydrogens of **6**) was fixed at 1.2 times the equivalent isotropic thermal parameter of the carbon atom to which it is covalently bonded.

Structural models that utilized anisotropic thermal parameters for all non-hydrogen atoms of both compounds and isotropic thermal parameters for all included hydrogen atoms were refined to convergence [*R*[25] = 0.042 (**5**) and 0.045 (**6**), R_w[25] = 0.048 (**5**) and 0.054 (**6**) for 2204 (**5**) and 2711 (**6**) independent absorption-corrected reflections having $I > 3\sigma(I)$] using counterweighted[24] full-matrix least-squares techniques.

All structure factor calculations for both compounds employed recent

---

(24) For counter weights: $\sigma_F = \{[\sigma(F_o)]^2 + (p|F_o|)^2\}^{1/2}$, where the "ignorance factor", *p*, has the value of 0.03 for both compounds.

(25) The *R* values are defined as $R = \sum||F_o| - |F_c|| / \sum|F_o|$ and $R_w = \{\sum w(|F_o| - |F_c|)^2 / \sum w|F_o|^2\}^{1/2}$, where $w = [\sigma(F)]^{-2}$ is the weight given each reflection. The function minimized is $\sum w(|F_o| - K|F_c|)^2$, where *K* is the scale factor.

tabulations of atomic form factors[26a] and anomalous dispersion corrections[26b] to the scattering factors of the Ru and P atoms. The final cycles of refinement for both compounds employed a least-squares refineable extinction correction.[27] All calculations were performed on a Data General Eclipse S200 or S-230 computer using versions of the Nicolet E-XTL or SHELXTL interactive crystallographic software package or on an IBM-compatible 486 personal computer using the Siemens SHELXTL-PC interactive software package.

Final atomic coordinates, anisotropic thermal parameters for non-hydrogen atoms, and bond lengths and angles in the anions, cations and solvent molecules of **5** and **6** are given with estimated standard deviations in Tables SI–SX.[15] Fractional atomic coordinates and relevant bond lengths and angles for the anions of **5** and **6** are given with estimated standard deviations in Tables II–V.

Acknowledgment. W.G.K., R.P.P., A.Y., and B.Z. are grateful to the National Science Foundation for financial support. Scott Wilson of the University of Illinois School of Chemical Sciences X-ray Crystallographic Laboratory performed the structure determination of compound **6**.

Supplementary Material Available: Tables of crystal structure reports, complete atomic coordinates and anisotropic thermal parameters, and complete bond lengths and angles for non-hydrogen atoms and ORTEP plots for anions, cations, and solvent molecules of crystallization for $[(CH_3CN)_3Ru(P_3O_9)][N(C_4H_9)_4]\cdot CH_3CN$ (**5**) and $[(C_8H_{12})Ru(NH_2NC(CH_3)_2)(P_3O_9)][N(C_4H_9)_4]\cdot CH_3COCH_3$ (**6**) (37 pages). Ordering information is given on any current masthead page.

---

(26) *International Tables for X-Ray Crystallography*; Kynoch: Birmingham, England, 1974; Vol. IV: (a) pp 99–101; (b) pp 149–150; (c) pp 55–66.

(27) Larson, A. *Acta Crystallogr.* **1967**, *23*, 664.

(28) *International Tables for X-Ray Crystallography*; Kynoch: Birmingham, England, 1969; Vol. I.: (a) p 115; (b) p 75.